

An alternative way of looking at our results is in terms of the purity of the cesium ground state. If some p state is present so that the wave function takes the form $|s\rangle + a|p\rangle$, then the dipole moment of the atom is given by

$$d_A = -e\langle s|\vec{r}|p\rangle(a + a^*), \quad (4)$$

where we have adopted the phase convention in which the matrix element of r is real. We assume that any admixture is due to an internal interaction within the atom. Such an interaction must violate parity in order to admix a p state into an s state. It must also violate time-reversal invariance in order to ensure that the admixture coefficient a is real; otherwise the dipole moment will vanish. From our measured limit on the edm of the atom we deduce that

$$|a| \leq 2 \times 10^{-12},$$

where we have obtained a rough value of the matrix element of r from the atomic polarizability.¹¹ To illustrate the order of magnitude of this limit, we calculate the admixture of p state into the ground s state in cesium that one would expect due to parity-nonconserving weak interactions. Carhart¹² has calculated the admixture of $2p$ state into the $2s$ state of hydrogen. His theory can readily be applied to cesium, and we find $|a| \approx 10^{-12}$. This admixture is pure imaginary so that $a + a^* = 0$, and the edm is zero as it must be since Car-

hart's theory is time-reversal invariant. Nonetheless, the fact that weak interactions can produce admixtures of the same order as our experimental limits suggests that if time-reversal invariance is violated in the weak interactions a measurable edm of the cesium atom might result.

The authors wish to acknowledge the help of Mr. John Carrico who aided with much of the data taking.

*Work supported by the National Science Foundation.

†Permanent address: Clarendon Laboratory, Oxford, England.

¹L. Landau, Nucl. Phys. 3, 127 (1957).

²T. D. Lee and C. N. Yang, Brookhaven National Laboratory Report No. BNL-443 (F91), October 1957, p. 17 (unpublished).

³J. H. Christenson, J. W. Cronin, V. L. Fitch, and R. Turlay, Phys. Rev. Letters 13, 138 (1964).

⁴M. Sachs and S. L. Schwebel, Ann. Phys. (N.Y.) 6, 244 (1959); 8, 475 (1959).

⁵M. E. Browne, Phys. Rev. 121, 1699 (1961).

⁶E. Lipworth, S. Legowski, and P. G. H. Sandars, Bull. Am. Phys. Soc. 9, 91 (1964).

⁷L. I. Schiff, Phys. Rev. 132, 2194 (1963).

⁸E. E. Salpeter, Phys. Rev. 112, 1642 (1958).

⁹P. G. H. Sandars, to be published.

¹⁰J. Goldemberg and Y. Torizuka, Phys. Rev. 129, 2580 (1963).

¹¹G. E. Chamberlain and J. C. Zorn, Phys. Rev. 129, 677 (1963).

¹²R. A. Carhart, Phys. Rev. 132, 2337 (1963).

MULTIMODE EFFECTS IN STIMULATED RAMAN EMISSION

N. Bloembergen* and Y. R. Shen

Department of Physics, University of California, Berkeley, California

(Received 19 November 1964)

The multimode structure of high-power Q -switched lasers has been shown to have an important effect on the second-harmonic generation of light.¹ The present note calls attention to the even more pronounced effects of the spatial and temporal distribution of the laser modes on the stimulated Raman emission.

Consider the generation of Stokes radiation by two laser modes, represented by plane waves at the same frequency ω_L but traveling in slightly different directions. The wave vectors are denoted by \vec{k}_L and \vec{k}_L' , with corresponding complex amplitudes E_L and E_L' . The usual notion is that the gain for each mode at the Stokes fre-

quency is proportional to the laser intensity $|E_L|^2 + |E_L'|^2$. Consider, however, the pair of Stokes modes for which $\vec{k}_L - \vec{k}_S = \vec{k}_L' - \vec{k}_S'$. The coupled amplitude equations² describing the growth of these modes are

$$\begin{aligned} dE_S/dz &= C \{|E_L|^2 + |E_L'|^2\} E_S + CE_L^* E_L' E_S', \\ dE_S'/dz &= CE_L' E_L^* E_S + C \{|E_L|^2 + |E_L'|^2\} E_S', \end{aligned} \quad (1)$$

where the constant C is related to the Raman susceptibility at resonance $\chi_S''(0)$ by

$$C = (2\pi\omega_S^2/c^2 k_{zS}) |\chi_S''(0)|. \quad (2)$$

The eigenvalues of the imaginary part of the propagation vector, or the exponential gain constant g_S , are given by

$$g_S = C \{ |E_L|^2 + |E_L'|^2 \pm |E_L E_L'| \}. \quad (3)$$

For $|E_L| = |E_L'|$ the coupled Stokes mode with a ratio of the complex amplitudes $E_S/E_{S'}$ = $\exp[i(\varphi_L - \varphi_L')]$, or $|E_S| = |E_{S'}|$ and $\varphi_{S'} - \varphi_S = \varphi_L' - \varphi_L$, has a gain which is 1.5 times the average gain, or three times larger than the other mode for which $|E_S| = |E_{S'}|$, but $\varphi_{S'} - \varphi_S = \pi + (\varphi_L' - \varphi_L)$. The physical meaning is clear: If the two original Stokes modes interfere constructively in the same region in which the laser modes interfere constructively, a larger gain results.

It is possible to extend this consideration to pairs of Stokes modes which have exact momentum matching in the transverse direction, but have a small mismatch along the z direction which may be taken along \vec{k}_L . The vector \vec{k}_L' makes an angle θ_L' and \vec{k}_S and angle θ_S with the z direction. Let $\vec{k}_{S'}$ be the vector of a Stokes mode that preserves transverse momentum, $k_S(\sin\theta_{S'} - \sin\theta_S) = k_L \sin\theta_L'$; then if the mismatch along the z direction is given by a simple geometrical consideration,

$$\begin{aligned} \Delta k_z &= k_{S_z'} + k_{L_z'} - k_L - k_{S_z} \\ &= \frac{1}{2} \theta_L' k_L (\theta_S' + \theta_S - \theta_L'). \end{aligned} \quad (4)$$

For $\theta_L' \sim 10^{-3}$ and $\theta_S \sim 10^{-2}$ radian, the waves remain in phase for about 5 to 10 cm. Therefore, Stokes radiation within 0.5° of the forward or backward direction can take full advantage of the increased gain over this length, if the laser power is divided over two modes.

Consider next N spatial laser modes at the same frequency. The N modes may be represented by plane waves passing through an area A into a solid angle $d\Omega_L$, $N = A\lambda_L^{-2} d\Omega_L$. A pair of Stokes waves with propagation vectors \vec{k}_S and $\vec{k}_{S'}$ is coupled together by a term $C \sum_i \sum_j E_{L,i} E_{L,j}^* \delta(\Delta k_x) \delta(\Delta k_y)$. The δ functions insure transverse momentum matching, e.g., $\Delta k_x = k_{L,i,x} - k_{L,j,x} + k_{S,x} - k_{S',x} = 0$. A large number of Stokes modes are thus coupled together, leading to a determinantal problem of high order. The coupled modes with the largest roots for the gain constant are of most interest. The average gain for all modes is equal to the usual value $C \sum_j |E_{L,j}|^2$, as follows immediately from the trace.

Assume that the N laser waves have equal amplitudes, but statistically independent, uniformly distributed random phases. This model may not be a good approximation for the field from a high-powered laser, but it allows the calculation of a definite result to illustrate the basic idea. Cut the cross section of the beam into N elements, $dA_i = A/N$. The amplitude of the laser field in this element will be given by the two-dimensional random walk of N steps. If N is large, the intensity distribution over the cross section will be given by an exponential function. Consider the linear combination of Stokes waves that peaks the amplitude in the same element dA_i , where the laser amplitude has a maximum. This coupled Stokes mode will have maximum gain. The distribution function of the Stokes gain is also given by an exponential law in this model,

$$w(g_S) dg_S = (C \sum |E_{L_j}|^2)^{-1} \exp(-g_S / C \sum |E_{L_j}|^2) dg_S.$$

The probability to have at least one normal mode with a gain coefficient larger than the average gain by a factor $\ln N$ is $1 - e^{-1} = 0.63$. The observed Stokes intensity will arise predominantly from the few modes with an exceptionally large gain constant. The waves in the Stokes oscillator have an almost uncanny ability to match their relative phases to those that happen to be present in the laser waves to maximize the gain. In a Stokes amplifier the relative phases in the input are in general not so accommodated. The initial gain in a Stokes amplifier will be well represented by the average value with statistical fluctuations around it. The initial gain in a Stokes oscillator is higher by a factor $\ln N$, which lies between 4 and 8 for 10^2 to 10^3 laser modes. This enhanced gain will fade away after about 5-10 cm path length because then the favorable phase relationships are lost according to Eq. (4). Optical inhomogeneities may also be expected to become an important factor over about the same length.

It is believed that the multimode structure is the reason for the sharp peaking of the Stokes intensity in the forward direction. Geometrical factors are not sufficient to explain this, nor the fact that it is an order of magnitude more difficult to construct a Raman laser with the Stokes beam going in a different direction than the the laser beam.³ In this case relative phase matching and the beneficial factor $\ln N$

does not apply, as Eq. (4) indicates that for θ_S the phase mismatch $\exp(i\Delta kz)$ averages out the cross-coupling terms.

The most striking experimental evidence comes, however, from experiments by Lallemand⁴ and by Bret.⁵ They have shown independently that the gain per unit length in a first Raman cell of 10-cm length is much higher than in subsequent cells used as amplifiers. The gain decreases but does not completely saturate. No significant depletion of the laser power occurs. These results are consistent with the multimode picture.

The objection may be raised that large deviations from the average laser intensity over the cross section are not observed. The intensity pattern will, however, change many times during a giant laser pulse of duration t_p . Even for a spectral distribution as narrow as 0.005 cm^{-1} and a pulse as short as 10^{-8} sec, the number of different temporal modes $\Delta\omega t_p$ is about 10. The intensity integrated over the pulse

$$\left\{ \frac{2\pi i(\omega_S + n\Delta)^2}{c^2 k_{S, n\Delta}} \right\}^{-1} \frac{dE_{S, n\Delta}}{dz} = \{ \chi_S(n\Delta) |E_L|^2 + \chi_S(n\Delta - \Delta) |E_{L, \Delta}|^2 \} E_{S, n\Delta} + \chi_S(n\Delta) E_L^E E_{L, \Delta}^* E_{S, (n+1)\Delta} + \chi_S(n\Delta - \Delta) E_L^* E_{L, \Delta}^E E_{S, (n-1)\Delta}. \quad (5)$$

The strong dispersion in the Raman susceptibility makes it difficult to obtain a solution in closed form. Side bands generated by acoustic modulation of the optical index of refraction have been discussed by Brillouin and by Raman and Nath.⁶ In our case the presence of the laser components modulates the optical index at the difference frequency Δ . The problem is complicated by the variation of the complex coupling constant χ_S . It may be inferred from perturbation theory that the ratio of the amplitudes of successive Fourier components is approximately given by $|E_{S, n\Delta}/E_{S, (n-1)\Delta}| \sim |\chi_S(n\Delta)/\chi_S''(0)|$. For $\Delta > 0.1\Gamma$, the Fourier components will essentially have comparable intensity within the width of the resonance curve for $|\chi_S|$, which has a full width at half maximum of $2\sqrt{3}\Gamma$. In the wings the intensity will drop rapidly.

At the same time additional side bands are generated at the laser frequency. A component at $\omega_L + n\Delta$ is, for example, created by a nonlinear polarization $\chi(\Delta) E_{L, \Delta}^E E_{S, (n-1)\Delta}^*$. These new Fourier components have about the same intensity and the same angular distribu-

tion as the corresponding Stokes components.

Turning from the spatial to the temporal distribution of modes, consider the case that the laser intensity contains two well-separated frequency components with well-defined phases, E_L and $E_{L, \Delta}$. The frequency spacing Δ is supposed to be a fraction of the Raman linewidth Γ . One might think that the laser lines would generate a single sharp Stokes line at $\omega_L + \frac{1}{2}\Delta - \omega_{\text{vib}}$ by Raman laser action, because the vibrational level is homogeneously broadened. It is easy to show, however, that a mixed mode containing two frequencies, $\omega_S = \omega_L - \omega_{\text{vib}}$ and $\omega_S + \Delta$, will have a larger exponential gain, by an analysis similar to that contained in Eqs. (1)-(3). One can do still better by also admixing Fourier components at $\omega_S \pm n\Delta$ with properly chosen relative phases. Introduce the notation $\chi_S(n\Delta)$ for the complex Raman susceptibility with an offset $n\Delta$ from exact resonance. The component at $\omega_S + n\Delta$ is coupled by the relation

tion as the corresponding Stokes components.

Although the Stokes intensity seldom amounts to more than 10% of the original laser intensity, it is nevertheless always sufficient to create several higher orders of Stokes lines at $\omega_L - 2\omega_{\text{vib}}$, etc. The effectiveness of the Stokes light as a pump is probably due to its multimode character. The number of Stokes modes excited will usually be larger than 10^6 . This increases the maximum second-order Stokes gain by a factor $\ln N \sim 15$ to 20.

The generation of anti-Stokes radiation is coupled to that of Stokes radiation in a mode with mixed character and exponential gain.⁷ This coupling is only strong near the condition of momentum matching. Side bands near the anti-Stokes frequency will also be admixed. The frequency component $\omega_a + n\Delta$ is, for example, coupled by a nonlinear polarization $\chi_a E_L^E E_{L, \Delta}^E E_{S, (n-1)\Delta}^*$. This component is attenuated by the degenerative diagonal terms $-|\chi_a''(n\Delta)| |E_L|^2 E_{a, n\Delta} - |\chi_a''(n\Delta - \Delta)| |E_{L, \Delta}|^2 \times E_{a, n\Delta}$. Since the imaginary part drops rapidly away from resonance, the generation of

anti-Stokes frequencies in the wings of the resonance is relatively favored.⁸ The component $\omega_a + n\Delta$ can also be generated by terms of the form $\chi(0)E_L E_S^* E_{L, n\Delta} + \chi(\Delta)E_L E_{S, \Delta}^* E_{L, n\Delta - \Delta}$, etc. The magnitude of this term is comparable to the terms involved in the generation of second-order Stokes radiation. The momentum-matching condition also favors this path for the creation of anti-Stokes intensity, as illustrated in Fig. 1. Because $k_{L, n\Delta}$ may make an angle θ with k_L , it is possible to choose a Stokes direction about 0.5θ closer to k_L . Because the Stokes intensity drops rapidly with increasing θ , this choice increases the coupling with the corresponding anti-Stokes component considerably. It is emitted in a cone with an apex half-angle $\theta_0 + \frac{1}{2}\theta$, where θ_0 is the phase-matched angle for a strictly parallel laser beam. This mechanism can thus account for rather broad anti-Stokes cones with the center of gravity occurring at an angle considerably larger than θ_0 . The magnitude $\frac{1}{2}\theta$ may vary between 0.2° and about 1° . Such features have been reported by several workers.⁹ It also accounts for the dark absorption¹⁰ at ω_a , because this frequency is most strongly attenuated in all directions, except near θ_0 .

The anti-Stokes intensity is sufficient to create in turn several higher order anti-Stokes components, $\omega_{aa} = \omega_L + 2\omega_{\text{vib}}$, etc. Again the multimode effect will increase the effectiveness of these conversions. Their frequency distribution will be determined by successive convolutions of the original frequency distributions. The component $\omega_{aa} + 2n\Delta$ may, for example, be created by a nonlinear polarization $\chi(n\Delta) \times E_{a, n\Delta} E_L E_{S, -n\Delta}^*$ and a component at $\omega_{aa} + 3n\Delta$ by $\chi(2n\Delta) E_{a, n\Delta} E_{L, n\Delta} E_{S, -n\Delta}^*$. There are many other possible combinations. The broadening of higher order Stokes lines proceeds in a similar manner. Since usually three or more orders of Stokes and anti-Stokes lines are observed, the beating back and forth between the various orders occurs about four times. A total width of the frequency distribution of

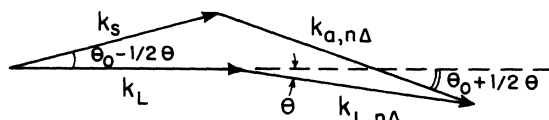


FIG. 1. An effective path for anti-Stokes generation. New parametrically generated components near the laser frequency are used, as explained in the text.

$4 \times 2\sqrt{3}\Gamma$ may be expected. With $\Gamma = 3 \text{ cm}^{-1}$ for nitrobenzene, this leads to a total width, measured between points of half-maximum intensity, of about 40 cm^{-1} . The detailed shape of the spectral distribution depends in an intricate manner on the interference of parametric coupling terms between many modes. The observed asymmetry in the distributions may be caused by the asymmetry in $|\chi_S|$, due to the contribution of the nonresonant part of the nonlinear susceptibility.

Stoicheff¹⁰ reported frequency distributions in essential accord with these considerations, when the laser pulse in his experiments contained two strong frequency components with a spacing $\Delta = 0.8 \text{ cm}^{-1}$. Without special precautions most high-powered laser pulses will contain several frequency components in an interval of about 1 cm^{-1} . This will cause an essentially continuous frequency distribution around the various Stokes and anti-Stokes frequencies.⁹ If the initial laser emission is narrower than 0.01Γ , the first-order Stokes broadening will not be able to fill the width of the vibrational resonance Γ . In this case all distributions will remain narrow and the ideal case of stimulated Raman emission by a monochromatic laser is approached.

The multimode structure of the laser beam seriously complicates the theoretical interpretation, because a very large number of waves has to be considered simultaneously. This semi-quantitative description of the characteristics of the solution provides a possible explanation for the many features of the observed spatial and frequency distributions in stimulated Raman emission. Since the multimode structure is different for different lasers and may vary from pulse to pulse, it accounts for the variety in detail reported by different workers. In particular, it highlights the difficulty in obtaining reliable quantitative values for the Raman susceptibility. The initial gain in a Raman oscillator free to choose the relative phases of its component modes can be much higher than in a Raman amplifier cell.

*On leave from Harvard University, Cambridge, Massachusetts.

¹J. Ducuing and N. Bloembergen, Phys. Rev. **133**, 1493 (1964).

²J. A. Armstrong, N. Bloembergen, J. Ducuing, and P. S. Pershan, Phys. Rev. **127**, 1918 (1962).

³H. Takuma and D. A. Jennings, Appl. Phys. Letters **4**, 185 (1964); J. H. Dennis and P. E. Tannen-

wald, Appl. Phys. Letters 5, 58 (1964).

⁴P. Lallemand, private communication.

⁵G. Bret, private communication.

⁶See, for example, M. Born and E. Wolf, Principles of Optics (Pergamon Press, London and New York, 1959), Chap. XII.

⁷N. Bloembergen and Y. R. Shen, Phys. Rev. Letters 12, 504 (1964).

⁸N. Bloembergen, Bull. Am. Phys. Soc. 9, 77 (1964).

⁹R. W. Terhune, Solid State Design 4, 38 (1964); H. J. Zeiger, P. E. Tannenwald, S. Kern, and R. Heerendeen, Phys. Rev. Letters 11, 419 (1963); R. W. Hellwarth, F. J. McClung, W. G. Wagner, and D. Weiner, Bull. Am. Phys. Soc. 9, 490 (1964); E. Garmire, *ibid.*

¹⁰B. Stoicheff, Phys. Letters 7, 186 (1963).

ATOMIC MASSES OF H¹, Cl³⁵, AND Cl³⁷†

Jay L. Benson and Walter H. Johnson, Jr.

School of Physics, University of Minnesota, Minneapolis, Minnesota

(Received 9 November 1964)

In this Letter we present the results of recent measurements of mass doublets which allow calculation of the mass of hydrogen and the two stable isotopes of chlorine. The measurements were made on the 16-inch mass spectrometer at the University of Minnesota¹ with a recent refinement in the peak-matching technique. In this technique, the peak shapes of the two ion groups composing the mass doublet are digitized and stored in the memory of a digital-memory oscilloscope. By inverting the wave form of one ion group previous to storage, an error signal proportional to doublet mismatch grows in the oscilloscope memory. Use of this error signal improves the precision of matching approximately 10 times over the precision of our previous method, since the storage technique greatly improves the signal-to-noise ratio of an individual matching.

The major isotope of hydrogen is the most important secondary mass standard. Since the adoption of C¹² as the mass standard, there have been no mass spectroscopic determinations of the mass of hydrogen. Previous to the adoption of C¹² as a mass standard, the mass of hydrogen was determined together with a number of other secondary standards by means of a group of independent doublet measurements. The use of C¹² as a standard has now permitted the direct measurement of H¹ in a single doublet. The doublet measured for the determination of the hydrogen mass was C₁₁H₂₂-C₁₂H₁₀, which reduces to a measurement of 12 hydrogen atoms against one carbon atom. The ions for this doublet are molecular ions of the hydrocarbon compounds undecene and biphenyl, respectively. Choice of molecular ions eliminates a possible systematic error resulting from initial ion energy. The

result of the doublet measurement is $\Delta M = 0.0939027 \pm 4$ u. We have considered in this result the effect of differing atomic binding energy in the two molecules making up the doublet. This energy difference is estimated to be about 27 electron volts, less than $\frac{1}{10}$ of the quoted error, and has been thus neglected.

The value of the hydrogen mass calculated from this doublet is shown in Table I. Also shown are the values of a previous measurement on the same spectrometer at this laboratory,² as well as a value calculated from measurements obtained by Smith³ employing a mass synchronometer. The disagreement between the present value and the previous Minnesota values appears to be consistent with the finding of König, Mattauch, and Wapstra⁴ that the ratio of external error to internal error was 2.65 for doublets measured at the time the previous result was obtained. The values of König, Mattauch, and Wapstra⁴ and Mattauch, Thiele, and Wapstra⁵ are from consistent lists of nuclidic masses computed with least-squares methods from all significant experimental mass measurement and reaction data available in 1961 and 1963, re-

Table I. Hydrogen mass on scale C² = 12 u.

Present value	1.007 825 22 ± 3
Previous Minnesota value ^a	1.007 824 70 ± 20
Smith ^b	1.007 824 93 ± 30
König, Mattauch, and Wapstra ^c	1.007 825 22 ± 8
Mattauch, Thiele, and Wapstra ^d	1.007 825 19 ± 8

^aReference 1.

^bValue calculated from values given in reference 3 converted to C¹² scale, and errors multiplied by ratio of external-to-internal error as suggested by author.

^cReference 4.

^dReference 5.